Acta Materialia 144 (2018) 164–176

Contents lists available at ScienceDirect

Acta Materialia

journal homepage: www.elsevier.com/locate/actamat

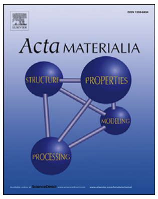

Full length article

Hydrogen-modified dislocation structures in a cyclically deformed ferritic-pearlitic low carbon steel

Shuai Wang [a, *], Akihide Nagao [b, c], Petros Sofronis [b, d], Ian M. Robertson [a, b, e, **]

[a] Department of Engineering Physics, University of Wisconsin-Madison, Madison, WI 53706, USA
[b] International Institute for Carbon-Neutral Energy Research (WPI-I2CNER), Kyushu University, 744 Moto-oka, Nishi-ku, Fukuoka, Fukuoka 819-0395, Japan
[c] Material Surface & Interface Science Research Department, Steel Research Laboratory, JFE Steel Corporation, 1-1 Minamiwatarida-cho, Kawasaki-ku, Kawasaki, Kanagawa 210-0855, Japan
[d] Department of Mechanical Science and Engineering, University of Illinois at Urbana-Champaign, Urbana, IL 61801, USA
[e] Department of Materials Science and Engineering, University of Wisconsin-Madison, Madison, WI 53706, USA

ARTICLE INFO

Article history:
Received 23 May 2017
Received in revised form
1 October 2017
Accepted 13 October 2017
Available online 28 October 2017

Keywords:
Hydrogen embrittlement
Fatigue
Low-carbon steel
Electron microscopy

ABSTRACT

The fatigue-crack growth rate of a ferritic-pearlitic low carbon steel was faster when the tests were conducted in high-pressure H_2 gas environments than in air. The predominant fracture feature changed from ductile fatigue striations with some "quasi-cleavage-like" regions when the test was conducted in air to mixed "quasi-cleavage" and "flat" facets when tested in a H_2 gas environment. The microstructure beneath the fracture surfaces produced in air was sub-grains, and over a distance of 15 μm from the fracture surface, the dimensions of the sub-grains increased. With hydrogen, dense dislocation bands and refined dislocation cells existed beneath the "quasi-cleavage" and "flat" fracture surfaces. The cell size increased with distance from the fracture surface. The decrease in the dimensions of the key microstructural features as the fracture surface is approached is attributed to the propagation of the crack through an already deformed matrix. The differences in evolved dislocation structure are explained in terms of the hydrogen-enhanced localized plasticity mechanism, and the hydrogen-modified dislocation structure establishes the local conditions that promote the fracture mode transition from ductile fatigue striations to a mixture of "quasi-cleavage" and "flat" features, which directly leads to enhanced fatigue-crack growth.

1. Introduction

The influence of hydrogen on the mechanical properties, including the fatigue properties, of metals is well established (see reviews by Murakami and Ritchie [1] and by Nanninga [2]). However, there remains debate about the mechanism associated with the hydrogen-induced failure, which in some systems can be accompanied by a change in the fracture path and mode. The prominent mechanisms used to explain hydrogen embrittlement include decohesion [3–5], hydrogen-enhanced localized plasticity (HELP) [6,7], hydrogen-enhanced vacancy production [8,9] and hydrogen-induced phase transformation [10–12]. Directly, linking these mechanisms, other than the one involving hydrides, to the actual hydrogen-induced failure remains a challenge.

In this study, a ferritic-pearlitic dual-phase low carbon steel was cyclically loaded in air and in gaseous hydrogen environments, the gas pressure was either 1 or 40 MPa. The presence of hydrogen, irrespective of the gas pressure, caused the crack-growth rate to increase by a factor of ≈12 at a stress-intensity factor range of $\Delta K = 25$ MPa $m^{½}$ and the fracture mode to change from being predominantly ductile fatigue striations with some regions exhibiting "quasi-cleavage-like" failure to being predominantly "quasi-cleavage" with some "flat" facets. The evolved microstructure as a function of distance from the fracture surface was examined using a scanning transmission electron microscope (STEM) to ascertain the mechanism responsible for the hydrogen-enhanced crack-growth rate and the transition in the fracture mode.

The basic tenet explored in this study is that the change in the fracture path and mode can be attributed to the influence of hydrogen on the deformation processes and that it is the different

---

* Corresponding author.
** Corresponding author. Department of Engineering Physics, University of Wisconsin-Madison, Madison, WI 53706, USA.
E-mail addresses: swang569@wisc.edu (S. Wang), irobertson@wisc.edu (I.M. Robertson).

https://doi.org/10.1016/j.actamat.2017.10.034
1359-6454/© 2017 Acta Materialia Inc. Published by Elsevier Ltd. All rights reserved.

fracture path and mode that account for the observed increase in crack-growth rate.

Roven and Nes have reviewed the evolution of the microstructure under controlled cyclic plastic strain [13] and fatigue-crack growth tests [14] of ferritic steel in the absence of hydrogen. At low and intermediate plastic strain levels, the evolved microstructure includes dislocation loops, veins, walls, persistent slip bands, labyrinths, cells, sub-grains, banded cells, and banded sub-grains. By increasing the cyclic strain to a higher level, the microstructure evolves to microbands, and non-crystallographic deformation bands, and grain boundaries can become displaced and serrated. In relating the striation formation to fatigue-crack propagation they suggested that the concept of one striation per load cycle is applicable over a narrow crack propagation rate interval, and that at a higher crack-growth rate the spacing between striations becomes independent of ΔK and more than one loading cycle is associated with the formation of each striation. It was proposed that fatigue-crack propagation is associated with a collapse of the dislocation microstructure at the crack tip. Hansen, Kuhlmann-Wilsdorf and co-workers have shown that the deformation microstructure can be classified as geometrically necessary boundaries, which include dense dislocation boundaries, microbands and lamellar boundaries, and incidental dislocation boundaries, which include dislocation cell walls and low-angle sub-grain boundaries [15–18]. Geometrically necessary boundaries are formed between regions in which different slip systems are activated and/or the magnitude of slip is different. These boundaries subdivide a grain and enclose a cell block, which is comprised of dislocation cell walls. The cell walls are composed of tangled dislocations and are formed in regions in which the same slip systems are active and the slip amplitude is similar. The morphology as well as the evolution of both the geometrically necessary boundaries and the incidental dislocation boundaries are dependent on the level of plastic strain. For example, the dimensions of dislocation cells decrease with increasing strain and then the misorientation angle between neighbouring cells increases as different slip systems are activated. Here the dislocation cells can transform to a sub-grain structure. This requires the reorganization and annihilation of dislocations to form the dislocation arrangements inside sub-grains and the sub-grain boundaries [15,17]. This study explores the effect of hydrogen on the organization of dislocations during cyclic loading and how it varies beneath different fracture surface features.

2. Experimental procedures

The chemical composition of the ferritic-pearlitic low carbon steel (JIS-SS400) used in this study is shown in Table 1. The steel plate of 19.0 mm thickness was manufactured by hot rolling. A round bar tensile specimen with a diameter and length of the reduced section of 6 mm and 3 mm, respectively, and a gage length of 24 mm, was machined from the middle thickness and parallel to the rolling direction of the plate. A uniaxial tension test was performed at an initial strain rate of $2.8 \times 10^{-3}\ \mathrm{s}^{-1}$ and yielded the following properties: lower yield strength = 314 MPa, upper yield strength = 339 MPa, ultimate tensile strength = 443 MPa, total elongation = 43.3% and reduction in area = 68.9%.

For the fatigue-crack growth test, compact tension (CT) specimens were prepared from the middle thickness of the plate in accordance with ASTM E647-08 standard with the crack-growth direction perpendicular to the rolling direction of the plate. The thickness of the CT specimen was 10.0 mm and the machined notch length was 10.3 mm from the line connecting the bearing points of force application. All the CT specimens were fatigue pre-cracked, $a_f = 1.7$ mm length, at a constant load ratio of $R = 0.1$, a frequency of $\nu = 5.0$ Hz, and $\Delta K = 21.35$ MPa m$^{1/2}$ at the interrupted position of $a = 12.0$ mm crack length at room temperature. The fatigue-crack growth tests were subsequently performed at $R = 0.1$ and $\nu = 1.0$ Hz at room temperature in air and in either a 1 or 40 MPa H_2 gas environment. Before the start of a fatigue test in H_2 gas, the specimen was held at the target H_2 gas pressure for 40 min. The crack-growth propagation tests were halted when ΔK reached 59.28 MPa m$^{1/2}$. In this study, the sample fatigued in air was used as a baseline rather than in vacuum as the emphasis was on comparing the dislocation microstructure evolved in a high-pressure gaseous hydrogen environment with that formed in air, which is the most common environment for fatigue-crack growth studies and also for industrial applications. Although conducting the fatigue tests in vacuum would have resulted in a longer fatigue life, a comparison of the evolved dislocation structures in copper tested in air and in vacuum to a comparable number of cycles exhibited no significant difference [19]. Furthermore, as will be demonstrated, the response of the samples tested in the different environments were significantly different.

Table 1
Chemical composition (mass%) of the JIS-SS400 steel investigated.

Element	C	Si	Mn	P	S	Cr	Al soluble	Total N	Fe
mass%	0.16	0.15	0.52	0.018	0.008	0.04	0.027	0.0036	Balance

The microstructure of the as-received steel in the undeformed state was evaluated using optical and transmission electron microscopy (TEM) techniques. For the optical microscopy, the surface was prepared by grinding, polishing, and etching (3% nital), and for the TEM analysis, a mechanically polished 100 μm-thick 3 mm diameter disc was thinned to electron transparency by twin-jet electropolishing using an electrolyte of 10% perchloric acid in ethanol under a voltage of 14 V and a temperature of −20 °C.

After the fatigue-crack growth tests, the fracture surfaces were first characterized by using a LEO 1530 field-emission scanning electron microscope (SEM). Then, samples were extracted from site-specific locations on the fracture surfaces and thinned to electron transparency using focused-ion beam (FIB) machining; this was performed using a Zeiss 1540XB Crossbeam workstation. A layer of Pt was deposited on the selected site to protect it during sample preparation. The sites for the observation of the fracture surfaces and their underlying microstructures were at either a ΔK value of 25 or 35 MPa m$^{1/2}$ and in the middle of the specimen thickness. The crack length at a ΔK of 25 and 35 MPa m$^{1/2}$ was 15.0 and 21.6 mm, respectively. The extracted foils were 20 μm wide along the fracture surface normal direction and 25 μm long in the crack propagation direction, and the thickness was between 200 and 300 nm.

Imaging of the defect microstructures was performed using a field emission scanning/transmission electron microscope (S/TEM, FEI Tecnai TF-30), which was operated at 300 kV. A zone-axis bright-field scanning transmission electron microscopy technique was used to observe and characterize the evolved microstructures [20].

The NanoMEGAS ASTAR automatic TEM phase-orientation mapping system attached to the Tecnai TF-30 S/TEM was used to generate orientation maps from regions containing dislocation cells, bands, and sub-grains; for details on the application of the ASTAR system see Refs. [21–23]. The precession electron diffraction (PED) technique with a precession angle of 0.8° allows for the reduction of electron diffraction dynamical effects and more accurate identification of crystallographic orientations. A scanning step of 5 nm was chosen for all scans. In this system, the diffraction patterns are compared to a library of known patterns, and the